Dyes and Pigments 91 (2011) 192–198

Contents lists available at ScienceDirect

Dyes and Pigments

journal homepage: www.elsevier.com/locate/dyepig

Organic dyes incorporating low-band-gap chromophores based on π-extended benzothiadiazole for dye-sensitized solar cells

Dong Hyun Lee [a], Myung Jun Lee [a], Hae Min Song [a], Bok Joo Song [a], Kang Deuk Seo [a], Mariachiara Pastore [b], Chiara Anselmi [b], Simona Fantacci [b,c], Filippo De Angelis [b], Mohammad K. Nazeeruddin [d], Michael Grätzel [d], Hwan Kyu Kim [a,*]

[a] Department of Advanced Materials Chemistry & Center for Advanced Photovoltaic Materials (ITRC), Korea University, ChungNam 339-700, Republic of Korea
[b] Istituto CNR di Scienze e Tecnologie Molecolari c/o Dipartimento di Chimica, Università di Perugia, via Elce di Sotto 8, I-06123 Perugia, Italy
[c] Italian Institute of Technology (IIT), Center for Biomolecular Nanotechnologies, Via Barsanti 73010, Arnesano, Lecce, Italy
[d] Laboratory for Photonics and Interfaces, Institute of Chemical Sciences and Engineering, Ecole Polytechnique Federale de Lausanne, 1015 Lausanne, Switzerland

ARTICLE INFO

Article history:
Received 1 February 2011
Received in revised form
9 March 2011
Accepted 9 March 2011
Available online 21 March 2011

Keywords:
Metal-free organic dyes
Low band-gap chromophore
Benzothiadiazole unit
Triphenylamine (TPA) unit
π-Bridge units
Dye-sensitized solar cells

ABSTRACT

A series of new π-conjugated organic dyes (HKK-BTZ1, HKK-BTZ2, HKK-BTZ3 and HKK-BTZ4), comprising triphenylamine (TPA) moieties as the electron donor and benzothiadiazole moieties as the electron acceptor/anchoring groups, was synthesized for the use in dye-sensitized solar cells (DSSCs). TPA units are bridged to benzothiadiazole with single(S), double(D) and triple bonds(T) in different derivatives. And HKK-BTZ1 was modified by introducing alkoxy group of TPA unit, because the bulky alkoxy group is a strong donating group for the more red shift and for reducing aggregation of dyes in TiO_2 film. The structure-property relationship was investigated. Under standard global AM 1.5 G illumination, a maximum photo-to-electron conversion efficiency of 7.30% was achieved with the DSSC based on dye HKK-BTZ4 ($J_{SC} = 17.9$ mA/cm^{-2}, $V_{OC} = 0.62$ V, FF = 0.66), while the Ru dye N719-sensitized DSSC showed an efficiency of 7.82% with a J_{SC} of 17.5 mA/cm^{-2}, a V_{OC} of 0.62 V, and a FF of 0.72.

1. Introduction

Over the last two decade, dye-sensitized solar cells (DSSCs), based on ruthenium complexes endowed with appropriate ligands and anchoring groups as the most widely used choice of charge transfer sensitizers for mesoscopic solar cells, have attracted significant attention as an alternative to the conventional solar cells due to their low-cost of production and high performance [1], since Grätzel and co-workers reported very high solar cell performances [2]. Several ruthenium-based sensitizers have achieved remarkable power conversion efficiency of 10-11% under standard global air mass 1.5 (AM 1.5G) illumination [3–5]. However, the rarity and high cost of the ruthenium metal may limit their development for large-scale applications. Consequently, many researchers have focused on developing metal-free organic sensitizers, and some of these endeavors have enhanced the solar-to-electric power conversion efficiencies reaching ca. 10% [6–10]. The advantages of organic dyes are: 1) easy preparation and purification, and lower cost, 2) they have higher molar absorption coefficients than the Ru(II) complexes, and 3) the wide variety of the structures and their facile modification provides potential for molecular design, with the introduction of substituents onto the chromophore skeletons allowing for easy control not only of their photophysical and electrochemical properties but also of their stereochemical structures [5–9]. Many organic dyes, based on the donor-(π-spacer)-acceptor (D-π-A) system, exhibiting relatively high DSSC performances, have so far been designed and developed. They include coumarin dyes [11–15]. triarylamine dyes [16–20], hemicyanine dyes [21,22], thiophene-based dyes [23], indoline dyes [24–30], heteropolycyclic dyes [31], porphyrin dyes [32–36], and phthalocyanine [37].

But, one of the main drawbacks of organic sensitizers is still the sharp and narrow absorption bands in the blue region of the visible region, impairing their light-harvesting capabilities. In this paper, we synthesized a series of new π-conjugated metal-free D-π-A organic dyes comprising triphenylamine (TPA) moieties as the electron donor and benzothiadiazole moieties as the electron acceptor/anchoring groups: First, the use of a π-extended benzothiadiazole derivative bridging unit between the TPA donor and the cyanoacrylic acid

* Corresponding author. Tel.: +82 41 860 1493; fax: +82 41 867 5396.
E-mail address: hkk777@korea.ac.kr (H.K. Kim).

0143-7208/$ – see front matter © 2011 Elsevier Ltd. All rights reserved.
doi:10.1016/j.dyepig.2011.03.015

anchoring group leads to higher efficiency, more red shift of absorption and emission bands than a D-π-A sensitizer based on benzothiadiazole (3.77%) reported by Ho and coworkers [38]. Second, the present π-extended BTZ dyes, associate with different links, such as single, double, and triple bonds have been designed and synthesized to investigate the structure-property relationship between the conversion efficiency and π-bridging system, which has not been well-established, yet [39–42]. Third, HKK-BTZ1 was modified by introducing alkoxy group of TPA donor unit onto triphenylamine unit, because the bulky alkoxy group is a strong donating group for reducing the gap between the HOMO and the LUMO resulting more red shift of the π–π* charge transfer transitions. Also, the branched alkoxy groups reduce aggregation of dyes in TiO_2 films.

2. Experimental

Details of the synthesis of the TPA donor and BTZ acceptor moieties are provided in the supplementary data.

2.1. Synthesis

2.1.1. 5-(7-(5-(4-(Diphenylamino)phenyl)thiophen-2-yl) benzo[c][1,2,5] thiadiazol-4-yl)thiophene-2-carb aldehyde (**15**)

A mixture of 2 (1.5 g, 3.68 mmol), 5-(7-(5-bromothiophen-2-yl) benzo[c][1,2,5]thiadiazol-4-yl)thiophene-2-carbaldehyde 12 (2.13 g, 7.37 mmol), $Pd(PPh_3)_4$ (0.15 g), Na_2CO_3 (0.5 g) was dissolved in toluene (50 mL)–EtOH (20 mL)–H_2O (20 mL) and the mixture was refluxed for 12 h. After evaporating the solvent under reduced pressure, H_2O (50 mL) and methylene chloride (50 mL) were added. The organic layer was separated and dried in $MgSO_4$. The solvent was removed under reduced pressure. The pure product 15 was obtained by column chromatography on silica gel using CH_2Cl_2. Yield: 35% (0.74 g, 1.3 mmol). ^{1}H-NMR (300 MHz; $CDCl_3$): $\delta = 9.97$ (s, 1H), 8.21–8.20 (d, 1H), 8.18–8.17 (d, 1H), 8.01–7.99 (d, 1H), 7.91–7.88 (d, 1H), 7.85–7.84 (d, 1H), 7.58–7.55 (d, 2H), 7.35–7.33 (d, 2H), 7.31–7.26 (m, 4H), 7.15–7.06 (m, 8H). MS-EI: m/z 571 (M^+). $\lambda_{max,abs}$ in THF: 365 nm, 516 nm. $\lambda_{max,em}$ in THF: 725 nm.

2.1.2. (2-Cyano-3-(5-(7-(5-(4-(diphenylamino)phenyl) thiophen-2-yl)benzo[c][1,2,5]thiadiazol-4-yl) thiophen-2-yl)acrylic acid) (***HKK-BTZ1***)

The compound **15** (0.2 g, 0.35 mmol), dissolved in $CHCl_3$ (20 mL), and acetonitrile (20 mL) was condensed with 2-cyanoacetic acid (0.044 g, 0.52 mmol) in the presence of piperidine (0.17 mL, 2.38 mmol). The mixture was refluxed for 18 h under a nitrogen atmosphere. After cooling to room temperature, the mixture was washed with 2 M aqueous HCl and extracted with $CHCl_3$. The solid was then washed with H_2O, dichloromethane, ethyl acetate and dried under vacuum for ca. 20 h to afford the product of **HKK-BTZ1** in 53% yield (0.12 g, 0.19 mmol). ^{1}H-NMR (300 MHz; $DMSO^d$): $\delta = 8.53$ (s, 1H), 8.35–8.33 (d, 2H), 8.31–8.30 (d, 1H), 8.25–8.24 (d, 1H), 8.21–8.18 (d, 1H), 8.11–8.09 (d, 2H), 7.71–7.68 (d, 2H), 7.60–7.59 (d, 2H), 7.38–7.33 (m, 4H), 7.13–7.07 (m, 6H), 7.03–7.00 (m, 2H). MS (MALDI-TOF): 638.1 (M^+). $\lambda_{max,abs}$ in THF:361 nm, 533 nm. $\lambda_{max,em}$ in THF:745 nm.

2.1.3. 5-(7-(5-(4-(Diphenylamino)styryl)thiophen-2-yl) benzo[c][1,2,5]thiadiazol-4-yl)thiophene-2-carbaldehyde (**16**)

A solution of tris(o-tolyl)phosphine (0.6 g, 0.03 mmol) and palladium acetate (0.03 g, 0.02 mmol) in dry DMF (150 mL) was added dropwise at 80 °C under a nitrogen atmosphere to a solution of 12 (1.98 g, 0.7 mmol), 4 (1.88 g, 1 mmol) in triethylamine (30 ml) and dry DMF (200 mL). After the mixture was heated at 110 °C for 12 h, the reaction mixture was poured into water (50 mL), and extracted with chloroform (40 mL × 3). The combined organic layers were neutralized with 1.2 N aqueous HCl 20 mL, washed with brine (30 mL × 3), dried over anhydrous magnesium sulfate, and evaporated in vacuum to dryness. The product 16 was purified by silica gelcolumn chromatograph. Yield: 12% (0.5 g, 0.84 mmol). ^{1}H-NMR (300 MHz; $CDCl_3$): $\delta = 9.97$ (s, 1H), 8.22–8.21 (d, 1H), 8.13–8.11 (d, 1H), 8.02–7.99 (d, 1H), 7.91–7.88 (d, 1H), 7.85–7.84 (d, 1H), 7.39–7.36 (d, 2H), 7.30–7.28 (m, 3H), 7.18–7.13 (m, 6H), 7.11–7.03 (m, 6H). MS-EI: m/z 597 (M^+). $\lambda_{max,abs}$ in THF:382 nm, 528 nm. $\lambda_{max,em}$ in THF:753 nm.

2.1.4. (2-Cyano-3-(5-(7-(5-((E)-4-diphenylamino)styryl) thiophen-2-yl)benzo[c][1,2,5]thiadiazol-4-yl) thiophen-2-yl)acrylic acid) (***HKK-BTZ2***)

The compound **16** (45 mg, 0.08 mmol), dissolved in $CHCl_3$ (20 mL) and acetonitrile (20 mL), was condensed with 2-cyanoacetic acid (9 mg, 0.52 mmol) in the presence of piperidine (0.04 mL, 0.51 mmol). The mixture was refluxed for 18 h. After cooling to room temperature, the mixture was washed with 2 M aqueous HCl and extracted with $CHCl_3$. The solid was then washed with H_2O, dichloromethane, ethyl acetate and dried under vacuum for ca. 20 h to afford the product of **HKK-BTZ2** in 53% yield (0.12 g, 0.18 mmol). ^{1}H-NMR (300 MHz; $DMSO^d$): $\delta = 8.46$ (s, 1H), 8.34–8.32 (d, 1H), 8.31–8.29 (d, 1H), 8.21–8.20 (d, 1H), 8.20–8.16 (d, 1H), 8.05 (s, 1H), 7.56–7.53 (d, 2H), 7.37–7.31 (m, 5H), 7.15–7.05 (m, 8H), 7.96–7.93 (d, 2H). MS (MALDI-TOF): 664.2 (M^+). $\lambda_{max,abs}$ in THF:391 nm, 546 nm. $\lambda_{max,em}$ in THF:760 nm.

2.1.5. 5-(7-(5-((4-(Diphenylamino)phenyl)ethynyl)thiophen-2-yl) benzo[c][1,2,5]thiadiazol-4-yl)thiophene-2-carbaldehyde (**17**)

The compound **7** (0.1 g, 0.37 mmol), 14 (0.18 g, 0.39 mmol), PPh_3 (1 mg, 0.004 mmol), $Pd(PPh_3)_2Cl_2$ (3 mg, 0.004 mmol), and CuI (1 mg, 0.01 mmol) were added into 20 ml solution (TEA:THF = 2:1). The mixture was stirred in a argon atmosphere under reflux for 24 h. After the solvent was removed by rotary evaporator, the residue was extracted with dichloromethane and water. The organic layer was dried with anhydrous magnesium sulfate overnight. The product was purified by silica gel column chromatograph (dichloromethane) Yield: 54% (0.12 g, 0.21 mmol). ^{1}H-NMR (300 MHz; $CDCl_3$): $\delta = 9.98$ (s, 1H), 8.22–8.21 (d, 2H), 8.07–8.06 (d, 1H), 8.02–7.99 (d, 1H), 7.91–7.88 (d, 1H), 7.85–7.84 (d, 1H), 7.39–7.36 (d, 2H), 7.33–7.31 (m, 4H), 7.29–7.27 (m, 4H), 7.14–7.05 (m, 7H), 7.03–7.00 (d, 2H). MS-EI: m/z 595 (M^+). $\lambda_{max,abs}$ in THF:362 nm, 496 nm. $\lambda_{max,em}$ in THF:721 nm.

2.1.6. (2-Cyano-3-(5-(7-(5-((4-(diphenylamino)phenyl)ethynyl) thiophen-2-yl) benzo[c] [1,2,5]thiadiazol-4-yl)thiophen-2-yl)acrylic acid) (***HKK-BTZ3***)

The compound **17** (180 mg, 0.3 mmol), dissolved in $CHCl_3$ (20 mL), and acetonitrile (20 mL), was condensed with 2-cyanoacetic acid (38 mg, 0.45 mmol) in the presence of piperidine (0.15 mL, 2.05 mmol). The mixture was refluxed for 18 h under a nitrogen atmosphere. After cooling to room temperature, the mixture was washed with 2 M aqueous HCl and extracted with $CHCl_3$. The solid was then washed with H_2O, dichloromethane, ethyl acetate and dried under vacuum for ca. 20 h to afford the product of **HKK-BTZ3** in 45% yield (0.09 g, 0.13 mmol). ^{1}H-NMR (300 MHz; $DMSO^d$): $\delta = 8.46$ (s, 1H), 8.36–8.34 (d, 1H), 8.32–8.31 (d, 1H), 8.29–8.26 (d, 1H), 8.20–8.18 (d, 1H), 8.06 (s, 1H), 7.52–7.51 (d, 2H), 7.47–7.44 (d, 2H), 7.41–7.35 (m, 4H), 7.18–7.10 (m, 6H), 6.92–6.89 (d, 2H). MS (MALDI-TOF): 662.1 (M^+). $\lambda_{max,abs}$ in THF:359 nm, 515 nm. $\lambda_{max,em}$ in THF:666 nm.

2.1.7. 5-(7-(5-(4(bis(4-(2-ethylhexyloxy)phenyl)amino)phenyl) thiophen-2 yl)benzo(c)[1,2,5]thiadiazole-4-yl)thiophene-2-carbaldehyde (**19**)

A mixture of 18 (1.11 g, 1.77 mmol), 12 (0.48 g, 1.18 mmol), $Pd(PPh_3)_4$ (0.05 g, 0.08 mmol), Na_2CO_3 (0.25 g, 2.36 mmol) was

dissolved in THF 50 mL, EtOH 20 mL, H_2O 20 mL and the mixture was refluxed for 12 h. After evaporating the solvent under reduced pressure, H_2O (50 mL) and methylene chloride (50 mL) were added. The organic layer was separated and dried in $MgSO_4$. The solvent was removed under reduced pressure. The pure product 19 was obtained by column chromatography on silica gel using CH_2Cl_2. Yield: 35% (0.74 g, 1.3 mmol). ^{1}H-NMR (300 MHz; $CDCl_3$): $\delta = 9.95$ (s, 1H), 8.18–8.16 (d, 1H), 8.15–8.14 (d, 1H), 7.96–7.94 (d, 1H), 7.85–7.81 (d, 2H), 7.49–7.46 (d, 2H), 7.28–7.26 (d, 1H), 7.10–7.07 (m, 2H), 6.95–6.92 (d, 2H), 6.87–6.83(d, 4H), 3.83(d, 4H), 1.40 (m, 2H), 1.57–1.18 (m, 16H), 0.93 (t, 12H,).

2.1.8. (Z)-3-(5-(7-(5(-4(bis(4-(2-ethylhexyloxy)phenyl)amino) phenyl)thiophen-2-yl)benzo(c)[1,2,5] thiadiazol-4-yl)thiophene-2-cyanoacrylic cid (***HKK-BTZ4***)

The compound **19** (0.45 g, 0.54 mmol) dissolved in $CHCl_3$ 20 mL and acetonitrile 20 mL was condensed with 2-cyanoacetic acid (0.068 g, 0.8 mmol) in the presence of piperidine (0.31 mL, 3.69 mmol). The mixture was refluxed for 18 h under a nitrogen atmosphere. After cooling to room temperature, the mixture was washed with 2 M aqueous HCl and extracted with $CHCl_3$. The solid was then washed with H_2O, dichloromethane, ethyl acetate and dried under vacuum for ca. 20 h to afford a product **HKK-BTZ4** in 53% yield (0.12 g, 0.19 mmol). ^{1}H-NMR (300 MHz; DMSO^d): $\delta = 8.21$–8.08 (m, 4H), 7.82–7.78 (d, 1H), 7.61–7.52 (d, 2H), 7.50–7.44 (d, 1H), 7.11–7.01 (d, 4H), 6.69–6.88 (d, 4H), 6.82–6.76 (d, 2H), 3.83(d, 4H), 1.40 (m, 2H), 1.57–1.18 (m, 16H), 0.93 (t, 12H), MS (MALDI-TOF): 894.15 (M^+). $\lambda_{max,abs}$ in THF:378 nm, 542 nm. $\lambda_{max,em}$ in THF:740 nm.

2.2. Measurement

^{1}H NMR was recorded with the use of Varian Oxford 300 MHz spectrometer; chemical shifts were reported in ppm units with tetramethylsilane as an internal standard. Infrared spectra were measured on KBr pellets using a Perkin-Elmer Spectrometer. The mass spectra were taken by a JEOL JMS-AX505WA mass spectrometer. The absorption and photoluminescence spectra were recorded on a Perkin-Elmer Lambda 2S UV-visble spectrometer and a Perkin LS fluorescence spectrometer, respectively. Cyclic voltammetry was carried out with a Versa STAT3 (AMETEK). The cyclic voltammogram curves were obtained from a three electrode cell in 0.1 M $TBAPF_6$ in CH_3CN at the scan rate of 50 mV s^{-1}, using dye coated TiO_2 electrode as a working electrode and Pt wire counter electrode and Ag/AgCl (saturated KCl) reference electrode (+0.197 V vs NHE) and calibrated with ferrocene. All of the measured potentials were converted to the NHE scale. Photovoltaic data were measured using a 1000 W xenon light source (Oriel, 91193) that was focused to give 1000 W/m^2, the equivalent of one sun at Air Mass (AM) 1.5 G, at the surface of the test cell. The light intensity was adjusted with a Si solar cell that was double-checked with an NREL-calibrated Si solar cell (PV Measurement Inc.). The applied potential and cell current were measured using a Keithley model 2400 digital source meter. The current–voltage characteristics of the cell under these conditions were determined by biasing the cell externally and measuring the generated photocurrent. This process was fully automated using Wavemetrics software.

2.3. Fabrication of dye-sensitized solar cells

The preparation of TiO_2 electrodes and the fabrication of the sealed cells for photovoltaic measurement were performed by following the procedures previously reported by Grätzel and co-workers. Fluorine-doped tin oxide (FTO) glass plates (Pilkington TEC Glass-TEC 8, Solar 2.3 mm thickness) were cleaned in a detergent solution using an ultrasonic bath for 30 min and then rinsed with water and ethanol. Then, the plates were immersed in 40 mm

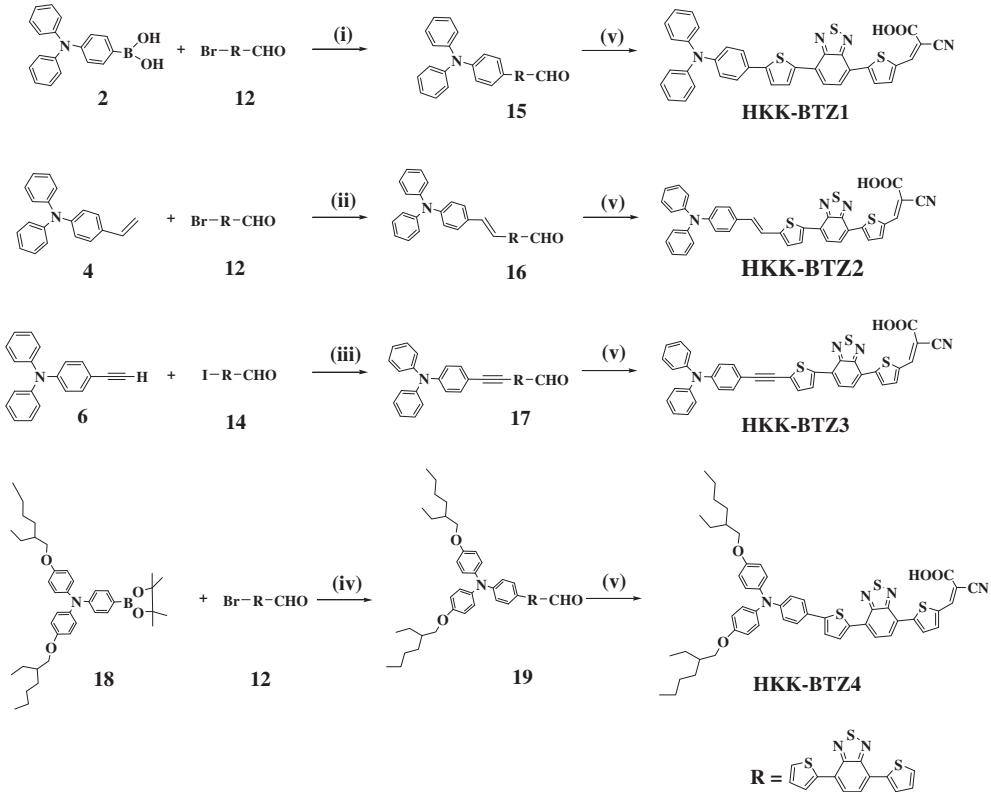

Scheme 1. Chemical structures and synthesis of **HKK-BTZ** dyes. (i) $Pd(PPh_3)_4$, Na_2CO_3, THF, Toluene; (ii) Tris(o-tolyl)phosphine, Pd(OAc), Triethylamine, DMF; (iii) $Pd(PPh_3)_2Cl_2$, CuI, PPh_3, Triethylamine; (iv)$Pd(PPh_3)_4$, Na_2CO_3, Toluene, EtOH; (v) Cyanoacetic acid, piperidine, $CHCl_3$, Acetonitrile).

$TiCl_4$ (aqueous) at 70 °C for 30 min and washed with water and ethanol. A transparent nanocrystalline layer was prepared on the FTO glass plates by a doctor blade method using TiO_2 paste (Solaronix, Ti-Nanoxide T/SP), which was then dried for 2 h at 25 °C. Then the TiO_2 electrodes were gradually heated under an air flow at 325 °C for 5 min, at 375 °C for 5 min, at 450 °C for 15 min, and at 500 °C for 15 min. The thickness of the transparent layer was measured by using an Alpha-step 200 surface profilometer (Tencor Instruments, San Jose, CA). A paste containing 400 nm sized anatase particles (CCIC, PST-400C) was deposited by means of doctor blade method on top of the transparent TiO_2 electrodes, to obtain a scattering layer. The deposited film then dried for 2 h at 25 °C. The TiO_2 electrodes were treated again with $TiCl_4$ at 70 °C for 30 min and sintered at 500 °C for 30 min. The resulting film was composed of 8 μm thick transparent layer and 8 μm thick scattering layer. The, films were immersed in dye solution (0.3 mM dye and 80 mM DCA in THF) of **HKK-BTZ1**, **HKK-BTZ-2**, **HKK-BTZ3** and **HKK-BTZ4** and kept at room temperature for 24 h. FTO plates for the counter electrodes were cleaned in an ultrasonic bath in H_2O, acetone, and 0.1 M aqueous HCl, respectively. The counter electrodes were prepared by placing a drop of an H_2PtCl_6 solution (2 mg Pt in 1 mL ethanol) on an FTO plate and heating it (at 400 °C) for 15 min. The dye-adsorbed TiO_2 electrodes and the Pt counter electrodes were assembled into a sealed sandwich-type cell by heating at 80 °C, using a hot-melt ionomer film (Surlyn) as a spacer between the electrodes. A drop of the electrolyte solution was placed in the drilled hole of the counter electrode and was driven into the cell via vacuum backfilling. Finally, the hole was sealed using additional Surlyn and a cover glass (0.1 mm thickness).

3. Results and discussion

Scheme 1 shows the synthetic protocol used for the π-extended BTZ dyes. The absorption, emission, and electrochemical properties of the **HKK-BTZ1-4** are listed in Table 1. Fig. 1 shows the UV–Vis spectra of the dyes in THF solutions, where the compounds exhibit two absorption maxima in regions of 361–378 nm and 533–542 nm, corresponding to triphenylamine unit to π-extended benzothiadiazole charge transfer transitions, respectively. It should be pointed out that their UV–visible absorption behavior was quite different from the similar dye structures based on fused thiophene derivatives with triphenlyamine unit [42]. It may indicate that the **HKK-BTZ 1-4** (D-π-A) organic dyes have a tilted structure between triphenylamine and π-extended benzothiadiazole units, yielding two strong absorption bands, which is in a good agreement with the result from

Table 1
Absorption, emission and electrochemical properties of the **HKK-BTZ** dyes.

Absorption			Emission	Electrochemical data		
Dye	λ_{max}[a]/nm (ε[b]/$M^{-1}cm^{-1}$)	λ_{max}[b]/nm (TiO_2)	λ_{max}[c]/nm	E_{Ox}[b]/V (vs NHE)	E_{0-0}[c]/V	E_{LUMO}[d]/V (vs NHE)
HKK-BTZ1	361(22047), 533(30791)	518	745	1.05	1.97	−0.92
HKK-BTZ2	391(20840), 546(23198)	528	760	0.93	1.93	−1.01
HKK-BTZ3	359(24651), 515(27169)	501	666	1.19	2.11	−0.92
HKK-BTZ4	378(22581), 542(31035)	525	740	0.98	1.93	−0.95

[a] Absorption was measured in THF solutions (1.0×10^{-5} M) at room temperature.
[b] The oxidation potential of the dye on TiO_2 was measured in acetonitrile with 0.1 M $TBAPF_6$ with a scan rate between 50 mV s^{-1} (working electrode and counter electrode: Pt wires, and reference electrode: Ag/AgCl).
[c] E_{0-0} was determined from intersection of absorption and emission spectra in THF.
[d] LUMO was calculated by $E_{ox}-E_{0-0}$.

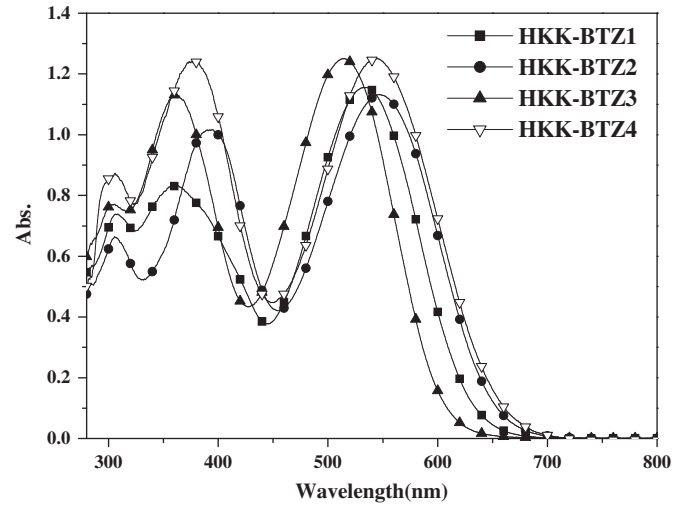

Fig. 1. Absorption spectra of **HKK-BTZ** dyes in THF at room temperature (conc. = 1.0×10^{-5} M).

DFT calculation. The UV/visible spectrum of **HKK-BTZ1** displays two absorption maxima at 533 nm ($\epsilon = 30{,}791$ dm^3 mol^{-1} cm^{-1}) and 361 nm, which are assigned as the π–π* transitions of the conjugated system. When a triphenylamine unit is bridged to benzothiadiazole with a double bond, the absorption maximum is red-shifted and the ϵ value is decreased compared to the **HKK-BTZ1** dye that has a single bond. Also, the absorption maximum of **HKK-BTZ3** that contains a triple bond is blue-shifted relative to **HKK-BTZ1** and **HKK-BTZ2** sensitizers. This may be attributed to the fact that, in the alkene bridged chromophores, all the carbon atoms on the branches are sp^2 hybridized to give a relatively longer conjugation. However, in the case of the alkyne chromophores, the carbon atoms are in both sp and sp^2 hybridized. This results in poorer π-orbital overlap and mismatch in energy of the π-orbitals, leading to a blue shift [43,44]. **HKK-BTZ4** dye with bulky alkoxy group was red-shifted, compared to **HKK-BTZ1**, due to the strong donating ability of the bulky alkoxy group. The donating effect has the more influence on triphenylamine unit rather than the benzothiadiazole unit, due to the direct attachment of the bulky alkoxy group onto triphenylamine unit, resulting in more red-shift.

Electrochemical properties of the **HKK-BTZ1**, **HKK-BTZ2**, **HKK-BTZ3**, and **HKK-BTZ4** were scrutinized by cyclic voltammetry in acetonitrile with 0.1 M tetrabutylammonium hexafluorophosphate by adsorbing onto TiO_2 films and the results are summarized in Table 1. The estimated LUMO of the **HKK-BTZ1**, **HKK-BTZ2**, **HKK-BTZ3**, and **HKK-BTZ4** from the oxidation potential and the energy at the intersection point of absorption and emission spectra are −0.92 V, −1.01 V, −0.92 V and −0.95 V vs NHE, respectively. Surprisingly, the LUMO level of **HKK-BTZ3** is lower than that of **HKK-BTZ2**, while the LUMO level of **HKK-BTZ3** is expected to be higher than that of **HKK-BTZ2** as follows: The absorption maximum of **HKK-BTZ3** is blue-shifted relative to **HKK-BTZ2** sensitizer. It leads to a larger band-gap between HOMO and LUMO level, so that the LUMO level generally rises up and the HOMO level goes down further. By contrast, it may be ascribed to the more electron negativity of sp character in **HKK-BTZ3** than that of sp^2 character in **HKK-BTZ2**, leading to the lower LUMO level [45].

In addition, introducing the bulky alkoxy substituent has a strong influence on the ground-state oxidation potentials and HOMO potentials and HOMO but a small effect on the ground-state reduction potentials and LUMO. The strong influence on the HOMO by introducing a stronger donor narrows the energy-gap of organic

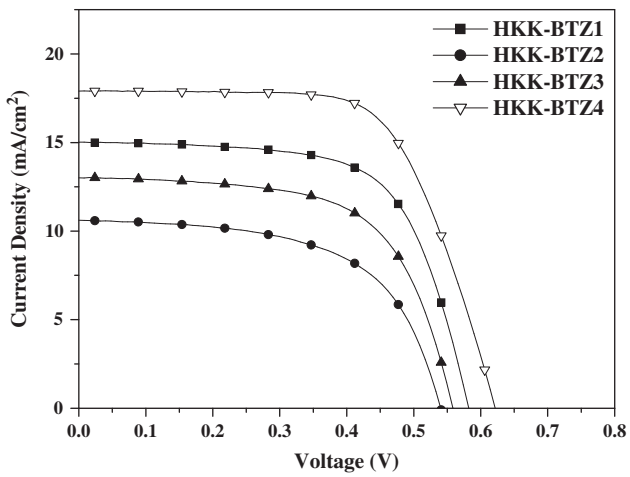

Fig. 2. Photocurrent–voltage characteristics of representative TiO_2 electrodes sensitized with **HKK-BTZ** dyes under AM 1.5 simulated sunlight (100 mW/cm^2).

sensitizers. **HKK-BTZ4** dye with bulky alkoxy group has the HOMO level of 0.98 V (vs NHE) and the LUMO level of −0.95 V (vs NHE). This is quite same from the previous result of the similar dye structures based on fused thiophene derivatives with triphenylamine unit reported by Peng group [42]. All LUMO are all higher than the conduction band edge of TiO_2 film, providing sufficient thermodynamic driving force for electron injection from the excited dyes to TiO_2 film.

The photovoltaic performance characteristics of **HKK-BTZ1- 4** were shown in Figs. 2 and 3. The incident monochromatic photon-to-current efficiency (IPCE) and current–voltage (J/V) characteristics were obtained with a sandwich cell comprising of 0.6 M 1,2-dimetyl-3-propyl imidazolium iodide, 0.05 M iodine, 0.1 M LiI, and 0.5 M tert-butylpyridine in acetonitrile. It was introduced into the inter-electrode space from the counter electrode side through predrilled holes. The drilled holes were sealed with a microscope cover slide and Surlyn to avoid leakage of the electrolyte solution. Typically, both the incident photon-to-electron conversion efficiency (IPCE) and the photocurrents in organic-based devices have been improved by the addition of deoxycholic acid (DCA) to break up dye aggregates [46–49]. Such an unwanted redox process is

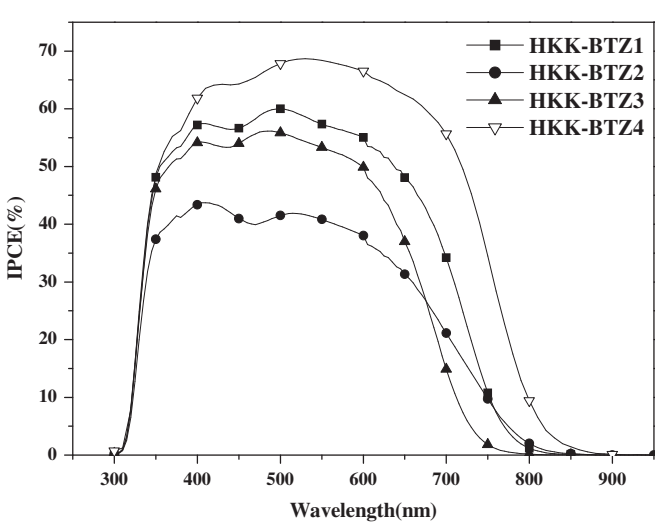

Fig. 3. Typical action spectra of incident photon-to-current conversion efficiencies (IPCE) obtained for nanocrystalline TiO_2 solar cells sensitized by **HKK-BTZ** dyes.

Table 2
Dye sensitized solar cell performance data of **HKK-BTZ** dyes.

Dye	DCA	J_{SC} (mA/cm^2)	V_{OC} (V)	FF	η (%)
HKK-BTZ1	0 mM	11.9	0.54	0.59	3.81
	40 mM	13.9	0.56	0.61	4.81
	80 mM	15.0	0.58	0.65	5.72
HKK-BTZ2	80 mM	10.6	0.54	0.59	3.37
HKK-BTZ3	80 mM	13.0	0.56	0.63	4.55
HKK-BTZ4	80 mM	17.9	0.62	0.66	7.30
N719	0 mM	17.2	0.71	0.72	8.97
	80 mM	17.5	0.62	0.72	7.82

TiO_2 thickness: 16 μm (8 μm + 8 μm: active layer + scattering layer); working area: 0.16 cm^2, electrolyte condition: 0.6 M DMPII, 0.1 M LiI, 0.05 M I_2, 0.5 M TBP in acetonitrile solution, 0.3 mM of dye was dissolved in THF.

retarded by the hydrophobic spacer and, as a result, the dark current is reduced and high open circuit voltage (V_{OC}) is obtained [50–53]. Table 2 shows the effect of the co-adsorbent DCA concentration on the **HKK-BTZ1** sensitized cell performance on under standard global AM 1.5 solar condition. As the co-adsorbent DCA concentration increases, the **HKK-BTZ1** sensitized cell performance enhances by slowing charge recombination, due to the prevention of dye aggregation [46,47]. At the co-adsorbent DCA concentration of 80 mM, the **HKK-BTZ1** sensitized cell gave a better result with the short circuit photocurrent density (J_{SC}) of 15.0 mA cm^{-2}, open circuit voltage (V_{OC}) of 0.58 V, and a fill factor (FF) of 0.65, corresponding to an overall conversion efficiency η of 5.72%, derived from the equation: $\eta = J_{SC}V_{OC}$FF/light intensity. Under the same conditions, the **HKK-BTZ2** sensitized cell gave a J_{SC} of 10.6 mA cm^{-2}, V_{OC} of 0.54 V, and a FF of 0.59, and the **HKK-BTZ3** sensitized cell gave a J_{SC} of 13.0 mA cm^{-2}, V_{OC} of 0.56 V, and FF of 0.63, corresponding to an overall conversion efficiency η of 3.37% and 4.55%, respectively. However, The IPCE data of **HKK-BTZ4** plotted as a function of excitation wavelength exhibits a wide wavelength over 800 nm.

The important red shift in the photocurrent response is attributed to the introduction of alkoxy group of TPA donor unit, because the bulky alkoxy group is a strong donating group for the more red shift and for reducing aggregation of dyes. The **HKK-BTZ4** sensitized cell under standard global AM 1.5 solar condition gave a J_{SC} of 17.9 mA cm^{-2}, V_{OC} of 0.62 V, and FF of 0.66, corresponding to an overall conversion efficiency η of 7.30%, while the Ru dye N719-sensitized TiO_2 showed an efficiency of 7.82% with a J_{SC} of 17.5 mA/cm^{-2}, a V_{OC} of 0.62 V, and a FF of 0.72, under the same DCA concentration of 80 mM (see Table 2).

To get a further insight into the difference in performance of DSSCs sensitized by all the dyes, density functional theory (DFT) calculations were performed at B3LYP/6-31G* level and at TDDFT calculations performed by MPW1 K/631G* in THF by means of CPCM model for the geometry optimization. The DFT/TDDFT calculations performed provide useful insights into the molecular and electronic structures of the dyes [54]. For **HKK-BTZ1**, we calculated (Table 3) absorption wavelenghts of 574 (protonated) and 544 nm (deprotonated) compared to the experimental value of 533 nm, possibly suggesting the dissociation of the cyanoacrylic

Table 3
Computed λ_{max} (nm), and HOMO/LUMO energies (eV) for the (a) protonated and (b) deprotonated **HKK-BTZ** dyes in THF.

Dye	λ_{max} (nm)	$\varepsilon_{HOMO}/\varepsilon_{LUMO}$ (eV)
HKK-BTZ1	574^a, 544^b	−5.66^b/−2.26^b
HKK-BTZ2	571	−5.54/−2.28
HKK-BTZ3	551	−5.69/−2.34
HKK-BTZ4	554	−5.50/−2.25

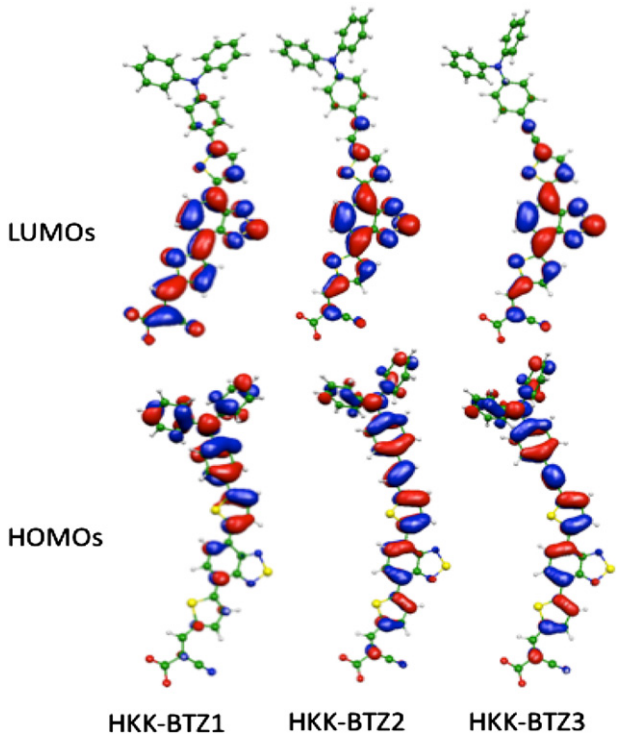

Fig. 4. Plots of the isodensity surfaces (MPW1K/6-31G* in THF) of HOMO and LUMO of **HKK-BTZ1**, **HKK-BTZ2** and **HKK-BTZ3**. (The HOMO and LUMO of **HKK-BTZ4** have the same spatial distribution of **HKK-BTZ1**.)

acid in THF. For the deprotonated **HKK-BTZ2** and **HKK-BTZ3** dyes, we obtained absorption maxima at 571 and 551 nm, respectively, which confirm the red-shifted absorption in **HKK-BTZ2** and the blue-shift in **HKK-BTZ3** compared to **HKK-BTZ1**, respectively. Introduction of O–R substituents to the TPA moiety of **HKK-BTZ1** leads in **HKK-BTZ4** to a slight red-shift of the absorption spectrum, perfectly in line with the experimental trend. This red-shift is essentially due to the TPA-based HOMO destabilization in **HKK-BTZ4**, due to the electron donating effect of the O–R substituents, while the LUMO energy is essentially unaltered, see Table 3. The optimized structures of the present dyes revealed that the introduction of both double and triple bonds forces the N-phenyl of TPA to be coplanar with the BTZ and cyanoacrylic units, while in **HKK-BTZ1** they are distorted by ca. 22°. Thus, the HOMO in **HKK-BTZ2** and **HKK-BTZ3** result to be delocalized from the donor to the acceptor (Fig. 4), reducing the effectiveness of charge separation and yielding to lower IPCE values and poorer performances.

4. Conclusions

A series of new π-conjugated metal-free organic dyes, comprising triphenylamine (TPA) moieties as the electron donor and benzothiadiazole moieties as the electron acceptor/anchoring groups, showed red-shift of absorption band in UV–visible spectrum because of long π conjugation and narrow band gap. The absorption maximum of the **HKK-BTZ2** dye with the double-bond bridged unit is red-shifted, compared to the **HKK-BTZ1** dye that has a single bond. Also, the absorption maximum of **HKK-BTZ3** that contains a triple bond is blue-shifted relative to **HKK-BTZ1** and **HKK-BTZ2** sensitizers. This may be due to the fact that, in the alkene chromophore, all the carbon atoms on the branches are sp^2 hybridized to give a relatively longer conjugation.

However, in the case of the alkyne chromophores, the carbon atoms are in both sp and sp^2 hybridized. It results in poorer π-orbital overlap and mismatch in energy of the π-orbitals, leading to a blue shift. Also, the D-π-A system shows easily polarizable and electron-deficient bridge between the push-pull chromophores. The photovoltaic performance based on the single-bond bridged unit in **HKK-BTZ1** dye is better than double and triple bond bridging, due to the higher charge separation. The introduction of bulky alkoxy group to TPA donor has a strong donating effect for the more red shift and for reducing aggregation of dyes. And the introducing of the bulky alkoxy substituent could lead to a fast dye-regeneration in order to avoid the geminate charge recombination between oxidized sensitizers and photoinjected electrons in the nanocrystalline TiO_2 film, thus enhancing the **HKK-BTZ1** sensitized cell performance.

The **HKK-BTZ4** sensitized cell under standard global AM 1.5 solar condition exhibited the better photovoltaic performance with J_{SC} of 17.9 mA cm^{-2}, V_{OC} of 0.62 V, and a FF of 0.66, corresponding to an overall conversion efficiency η of 7.30%, while the Ru dye N719-sensitized TiO_2 showed an efficiency of 7.82% with a J_{SC} of 17.5 mA/cm^{-2}, a V_{OC} of 0.62 V, and a FF of 0.72.

Acknowledgements

This work was supported by New & Renewable Energy Technology Development Program of the Korea Institute of Energy Technology Evaluation and Planning (KETEP) grant funded by the Korea government Ministry of Knowledge Economy (2010T100100674), WCU (the Ministry of Education and Science) program (R31-2008-000-10035-0) and Converging Research Center Program through the Ministry of Education, Science and Technology (2010K00973). FDA thanks Fondazione Istituto Italiano di Tecnologia – Project SEED 2009 – HELYOS for financial support.

Appendix. Supplementary data

Supplementary data associated with this article can be found in the online version, at doi:10.1016/j.dyepig.2011.03.015.

References

[1] Hagfeldt A, Grätzel M. Light-induced redox reactions in nanocrystalline systems. Chemical Reviews 1995;95:49–68.
[2] Grätzel M. Photoelectrochemical cells. Nature 2001;414:338–44.
[3] Nazeeruddin MK, Kay A, Rodicio L, Humphry-Baker R, Muller E, Liska P, et al. Conversion of light to electricity by cis-X2Bis(2,2′-bipyridyl-4,4′-dicarboxylate)ruthenium(II) charge-transfer sensitizers (X = $C1^-$ Br^- I^- CN^- and SCN^-) on nanocrystalline TiO_2 electrodes. Journal of American Chemical Society 1993;115:6382–90.
[4] Nazeeruddin MK, Péchy P, Renouard T, Zakeeruddin SM, Humphry-Baker R, Grätzel M, et al. Engineering of efficient panchromatic sensitizers for nanocrystalline TiO_2-based solar cells. Journal of American Chemical Society 2001; 123:1613–24.
[5] Ning Z, Fu Y, Tian H. Improvement of dye-sensitized solar cells: what we know and what we need to know. Energy & Environmental Science 2010;3: 1170–81.
[6] Mishra A, Fischer MKR, Bäuerle P. Metal-free organic dyes for dye-sensitized solar cells: from structure: property relationships to design rules. Angewandte Chemie International Edition 2009;48:2474–99.
[7] Ooyama Y, Harima Y. Molecular designs and syntheses of organic dyes for dye-sensitized solar cells. European Journal of Organic Chemistry; 2009: 2903–34.
[8] Zeng W, Cao Y, Bai Y, Wang Y, Shi Y, Wang P, et al. Efficient dye-sensitized solar cells with an organic photosensitizer featuring orderly conjugated ethylenedioxythiophene and dithienosilole blocks. Chemistry of Materials 2010; 22:1915–25.
[9] Im H, Kim S, Park C, Jang SH, Park NG, Kim C, et al. High performance organic photosensitizers for dye-sensitized solar cells. Chemical Communications 2010;46:1335–7.
[10] Seo SH, Kim SY, Koo BK, Cha SI, Lee DY. Influence of electrolyte composition on the photovoltaic performance and stability of dye-sensitized solar cells with multiwalled carbon nanotube catalysts. Langmuir 2010;26:10341–6.

[11] Hara K, Tachibana Y, Ohga Y, Shinpo A, Suga S, Arakawa H, et al. Dye-sensitized nanocrystalline TiO_2 solar cells based on novel coumarin dyes. Solar Energy Materials and Solar Cells 2003;77:89–103.
[12] Hara K, Sato T, Katoh R, Furude A, Ohga Y, Arakawa H, et al. Molecular design of coumarin dyes for efficient dye-sensitized solar cells. The Journal of Physical Chemistry B 2003;107:597–606.
[13] Furube A, Katoh R, Hara K, Sato T, Murata S, Tachiya M, et al. Lithium ion effect on electron injection from a photoexcited coumarin derivative into a TiO_2 nanocrystalline film investigated by visible-to-IR ultrafast spectroscopy. The Journal of Physical Chemistry B 2005;109:16406–14.
[14] Wang ZS, Cui Y, Hara K, Dan-oh Y, Kasada C, Shinpo A. A high-light-harvesting-efficiency coumarin dye for stable dye-sensitized solar cells. Advanced Materials 2007;19:1138–41.
[15] Seo KD, Song HM, Lee MJ, Pastore M, Gräetzel M, Kim HK, et al. Coumarin dyes containing low-band-gap chromophores for dye-sensitised solar cells. Dyes and Pigments 2011;90:304–10.
[16] Xu W, Peng B, Chen J, Liang M, Cai F. New triphenylamine-based dyes for dye-sensitized solar cells. The Journal of Physical Chemistry C 2008;112:874–80.
[17] Ning Z, Zhang Q, Wu W, Pei H, Liu B, Tian H. Starburst triarylamine based dyes for efficient dye-sensitized solar cells. The Journal of Organic Chemistry 2008; 73:3791–7.
[18] Li G, Jiang KJ, Li YF, Li SL, Yang LM. Efficient structural modification of triphenylamine-based organic dyes for dye-sensitized solar cells. The Journal of Physical Chemistry C 2008;112:11591–9.
[19] Wu W, Yang J, Hua J, Tang J, Zhang L, Tian H, et al. Efficient and stable dye-sensitized solar cells based on phenothiazine sensitizers with thiophene units. Journal of Materials Chemistry 2010;20:1772–9.
[20] Qu S, Wu W, Hua J, Kong C, Long Y, Tian H. New diketopyrrolopyrrole (DPP) dyes for efficient dye-sensitized solar cells. The Journal of Physical Chemistry C 2010;114:1343–9.
[21] Wang ZS, Li FY, Huang CH, Wang L, Wei M, Li NQ, et al. Photoelectric conversion properties of nanocrystalline TiO_2 electrodes sensitized with hemicyanine derivatives. The Journal of Physical Chemistry B 2000;104: 9676–82.
[22] Chen YS, Li C, Zeng ZH, Wang WB, Wang XS, Zhang BW. Efficient electron injection due to a special adsorbing group's combination of carboxyl and hydroxyl: dye-sensitized solar cells based on new hemicyanine dyes. Journal of Materials Chemistry 2005;15:1654–61.
[23] Tanaka K, Takimiya K, Otsubo T, Kawabuchi K, Kajihara S, Harima Y. Development and photovoltaic performance of oligothiophene-sensitized TiO_2 solar cells. Chemistry Letters 2006;35:592–3.
[24] Horiuchi T, Miura H, Uchida S. Highly efficient metal-free organic dyes for dye-sensitized solar cells. Journal of Photochemistry and Photobiology A: Chemistry 2004;164:29–32.
[25] Horiuchi T, Miura H, Sumioka K, Uchida S. High efficiency of dye-sensitized solar cells based on metal-free indoline dyes. Journal of American Chemical Society 2004;126:12218–9.
[26] Schmidt-Mende L, Bach U, Humphry-Baker R, Horiuchi T, Miura H, Grätzel M, et al. Organic dye for highly efficient solid-state dye sensitized solar cells. Advanced Materials 2005;17:813–5.
[27] Ito S, Zakeeruddin SM, Humphry- Baker R, Liska P, Charvet R, Grätzel, et al. High-efficiency organic-dye-sensitized solar cells controlled by nanocrystalline-TiO_2 electrode thickness. Advanced Materials 2006;18:1202–5.
[28] Howie WH, Claeyssens F, Miura H, Peter LM. Characterization of solid-state dye-sensitized solar cells utilizing high absorption coefficient metal-free organic dyes. Journal of American Chemical Society 2008;130:1367–75.
[29] Kuang D, Uchida S, Humphry-Baker R, Zakeeruddin SM, Grätzel M. Organic dye-sensitized ionic liquid based solar cells: remarkable enhancement in performance through molecular design of indoline sensitizers. Angewandte Chemie International Edition 2008;47:1923–7.
[30] Ito S, Miura H, Uchida S, Takata M, Sumioka K, Grätzel M, et al. High-conversion-efficiency organic dye-sensitized solar cells with a novel indoline dye. Chemical Communications; 2008:5194–6.
[31] Ooyama Y, Shimada Y, Kagawa Y, Imae I, Harima Y. Photovoltaic performance of dye-sensitized solar cells based on donor–acceptor π-conjugated benzofuro[2,3-c]oxazolo[4,5-a]carbazole-type fluorescent dyes with a carboxyl group at different positions of the chromophore skeleton. Organic & Biomolecular Chemistry 2007;5:2046–54.
[32] Imahori H, Umeyama T, Ito S. Large π-aromatic molecules as potential sensitizers for highly efficient dye-sensitized solar cells. Accounts of Chemical Research 2009;42:1809–18.
[33] Lu HP, Tsai CY, Yen WN, Hsieh CP, Yeh CY, Diau EWG, et al. Control of dye aggregation and electron injection for highly efficient porphyrin sensitizers adsorbed on semiconductor films with varying ratios of coadsorbate. The Journal of Physical Chemistry C 2009;113:20990–7.
[34] Imahori H, Matsubara Y, Iijima H, Umeyama T, Matano Y, Ito S, et al. Effects of *meso*-diarylamino group of porphyrins as sensitizers in dye-sensitized solar cells on optical, electrochemical, and photovoltaic properties. The Journal of Physical Chemistry C 2010;114:10656–65.
[35] Mai CL, Huang WK, Lu HP, Lee CL, Diau EWG, Yeh CY, et al. Synthesis and characterization of diporphyrin sensitizers for dye-sensitized solar cells. Chemical Communications 2010;46:809–11.
[36] Kang MS, Oh JB, Seo HD, Roh SG, Kim HK, Kim K, et al. Novel extended π-conjugated Zn(II)-porphyrin derivatives bearing pendant triphenylamine moiety for dye-sensitized solar cell: synthesis and characterization. Journal of Porphyrins and Phthalocyanines 2009;13:798–804.
[37] Eu S, Katoh T, Umeyama T, Matano Y, Imahori H. Synthesis of sterically hindered phthalocyanines and their applications to dye-sensitized solar cells. Dalton Transactions; 2008:5476–83.
[38] Velusamy M, Thomas KRJ, Lin JT, Hus YC, Ho KC. Organic dyes incorporating low-band-gap chromophores for dye-sensitized solar cells. Organic Letters 2005;7:1899–902.
[39] Teng C, Yang X, Yang C, Li S, Hagfeldt A, Sun L, et al. Molecular design of anthracene-bridged metal-free organic dyes for efficient dye-sensitized solar cells. The Journal of Physical Chemistry C 2010;114:9101–10.
[40] Teng C, Yang X, Yang C, Wang X, Hagfeldt A, Sun L, et al. Influence of triple bonds as π-spacer units in metal-free organic dyes for dye-sensitized solar cells. The Journal of Physical Chemistry C 2010;114:11305–13.
[41] Lu M, Liang M, Han HY, Sun Z, Xue S. Organic dyes incorporating bis-hexapropyltruxeneamino moiety for efficient dye-sensitized solar cells. The Journal of Physical Chemistry C 2011;115:274–81.
[42] Xu M, Li R, Pootrakulchote N, Shi D, Guo J, Wang P, et al. Energy-level and molecular engineering of organic D-π-A sensitizers in dye-sensitized solar cells. The Journal of Physical Chemistry C 2008;112:19770–6.
[43] Baek NS, Yum JS, Kim HK, Nazeeruddin MK, Grätzel M. Functionalized alkyne bridged dendron based chromophores for dye-sensitized solar cell applications. Energy & Environmental Science 2009;2:1082–7.
[44] Bhaskar A, Ramakrishna G, Lu Z, Twieg R, Hales JM, Goodson III T, et al. Investigation of two-photon absorption properties in branched alkene and alkyne chromophores. Journal of American Chemical Society 2006;128: 11840–9.
[45] Hagberg DP, Edvinsson T, Marinado T, Boschloo G, Hagfeldt A, Sun L. A novel organic chromophore for dye-sensitized nanostructured solar cells. Chemical Communications; 2006:2245–7.
[46] Wang P, Zakeeruddin SM, Humphry-Baker R, Grätzel M. A binary ionic liquid electrolyte to achieve ≥7% power conversion efficiencies in dye-sensitized solar cells. Chemistry of Materials 2004;16:2694–6.
[47] Kopidakis N, Neale NR, Frank AJ. Effect of an adsorbent on recombination and band-edge movement in dye-sensitized TiO_2 solar cells: evidence for surface passivation. The Journal of Physical Chemistry B 2006;110:12485–9.
[48] Wang P, Zakeeruddin SM, Comte P, Charvet R, Humphry-Baker R, Grätzel M. Enhance the performance of dye-sensitized solar cells by co-grafting amphiphilic sensitizer and hexadecylmalonic acid on TiO_2 nanocrystals. The Journal of Physical Chemistry B 2003;107:14336–41.
[49] Wang P, Zakeeruddin SM, Humphry-Baker R, Moser JE, Grätzel M. Molecular-scale interface engineering of TiO_2 nanocrystal: improving efficiency and stability of dye sensitized solar cells. Advanced Materials 2003;15:2101–4.
[50] Pelet S, Moser JE, Grätzel M. Cooperative effect of adsorbed cations and iodide on the interception of back electron transfer in the dye sensitization of nanocrystalline TiO_2. Journal of Physical Chemistry B 2000;104:1791–5.
[51] Hara K, Dan-oh Y, Kasada C, Ohga Y, Shinpo A, Arakawa H, et al. Effect of additives on the photovoltaic performance of coumarin-dye-sensitized nanocrystalline TiO_2 solar cells. Langmuir 2004;20:4205–10.
[52] Nazeeruddin MK, Péchy P, Renouard T, Zakeeruddin SM, Humphry-Baker R, Grätzel, et al. Engineering of efficient panchromatic sensitizers for nanocrystalline TiO_2-based solar cells. Journal of American Chemical Society 2001; 123:1613–24.
[53] Chiba Y, Islam A, Watanabe Y, Komiya R, Koide N, Han L. Dye-sensitized solar cells with conversion efficiency of 11.1%. Journal of Applied Physics 2006;45: L638–40.
[54] Geometry optimizations at B3LYP/6-31G* level and TDDFT calculations performed by MPW1K/631G* in THF by means of CPCM model.